

Article

Effect of Nanoplatelets Thickness on Photoluminescent, Optical, and Electronic Properties of Synthesized CdTe Semiconductor Nanoplatelets

Aizhan Akhmetova ^{*}, Asset Kainarbay ^{*}, Dulat Daurenbekov , Turlybek Nurakhmetov, Keleshek Zhangylyssov and Bagila Yussupbekova

Physics-Technical Faculty, L. N. Gumilyov Eurasian National University, 2 Satpayev Str., Astana Z01C0X0, Kazakhstan

^{*} Correspondence: aizhan.s.akhmetova@yandex.kz (A.A.); kainarbai_azh@enu.kz (A.K.)

Abstract: Quantum-confined CdTe nanoplatelets (NPL) are synthesized in colloidal solutions. The formation, growth, and transformation of 2D NPLs are monitored using UV-visible absorption PL spectroscopy and transmission electron microscopy. The luminescence intensity of NPL dependences on the temperature and injection of precursors is shown. It is found that the luminescence spectra shift to the long-wavelength region with increasing temperature due to an increase in the thickness of the NPL. The dependence of the band gap on the thickness of the NPL is shown. The band gap is determined by the thickness and number of layers. The dependence of the concentration of precursors in the reaction mass and the kinetics of NPL growth are shown. The excitation of defect states luminescence depends on the coordinating oleic ligand. The crystal structure of the CdTe NPL was analyzed via the electron diffraction pattern (ED), which allows a comparative conclusion about the crystal structure of the obtained NPL samples.

Keywords: semiconductor; 2D structure; CdTe; nanoplatelets; colloidal synthesis; electron diffraction



Citation: Akhmetova, A.; Kainarbay, A.; Daurenbekov, D.; Nurakhmetov, T.; Zhangylyssov, K.; Yussupbekova, B. Effect of Nanoplatelets Thickness on Photoluminescent, Optical, and Electronic Properties of Synthesized CdTe Semiconductor Nanoplatelets. *Crystals* **2023**, *13*, 1450. <https://doi.org/10.3390/cryst13101450>

Academic Editor: Ray-Hua Horng

Received: 31 August 2023

Revised: 23 September 2023

Accepted: 27 September 2023

Published: 29 September 2023



Copyright: © 2023 by the authors. Licensee MDPI, Basel, Switzerland. This article is an open access article distributed under the terms and conditions of the Creative Commons Attribution (CC BY) license (<https://creativecommons.org/licenses/by/4.0/>).

1. Introduction

Over the last few years, a new class of colloidal semiconductor quasi two-dimensional nanostructures called nanoplatelets (NPLs) has emerged. Atomically thin and flat two-dimensional CdSe nanoplatelets (NPLs) with a large lateral size have excited the research community [1]. These quasi-two-dimensional semiconductor NPLs strongly confine carriers. Since the thickness of NPLs can be controlled with atomic precision, these structures possess extremely narrow tunable absorption and emission bands. Due to their anisotropic shape, they exhibit a huge absorption cross section [2–5], increased energy transfer rates and optical gain [2], strongly anisotropic light emission [4–7], a high exciton binding energy level, and a high oscillator strength [1]. All these properties make semiconductor NPLs a potential candidate for low-gain lasing. The optical amplification threshold in NPLs is partially determined by the lifetime of several excitonic states [2]. Multiexcitons decay is caused predominantly by Auger recombination, where an electron–hole pair recombines without emission, exciting a third particle (electron or hole) to a higher energy level to conserve energy and momentum. The Auger biexciton lifetime increases linearly with an increasing lateral area of the NPL, but it strongly depends on the thickness. However, the nature and origin of the narrow exciton emission band of the NPL remains underexplored [3–5].

Cadmium telluride, a direct band gap A^{II}B^{VI} semiconductor with a zinc blende structure, is expected to have an even larger absorption cross section. Its optical absorption is mostly provided by the formation of free excitons [6]. The authors [7–9] studied the structural properties of cadmium tellurium nanocrystals. All these studies give a general idea about the relevance of the use of and research on cadmium telluride. Although there

are some comprehensive studies on the colloidal synthesis of CdTe quantum dots and nanorods [4,5,10–16], there are only a few reports on the synthesis of CdTe NPLs with a controlled shape due to the limited choice of tellurium precursors [17]. The authors of [18] studied the colloidal synthesis of wurtzite CdTe NPL using tributyl phosphine as a telluride precursor. They reported the colloidal synthesis of zinc blende CdTe NPLs using cadmium propionate or cadmium acetate as the cadmium precursor and TOP-Te (trioctylphosphine-tellurium) as the tellurium precursor. In this work, CdTe NPLs were synthesized at temperatures of 180 °C, 200 °C, and 250 °C, showing the possibility of increasing the NPL size by increasing the temperature and concentration of the metal precursor [4]. In [5], the authors studied spontaneous NPL folding by replacing oleic acid ligands with short-chain ones. The authors of [4] discovered that the film also has good photoconductivity properties.

The transverse size and shape of zincblende CdTe NPLs can be further controlled by changing the injection temperature or the molar ratio of oleic acid to a cadmium precursor with short-chain carboxylate groups. However, the mechanisms underlying the growth of CdTe NPLs are not fully understood [5,18,19].

Colloidal self-assembly is a powerful tool for controlling the orientation of building blocks in highly ordered functional materials [20–22].

The success of semiconductor QDs and NPLs is becoming increasingly important due to the fact that they indicate the application of nanotechnology in the fields of lasers, bioimaging, LEDs, and sensors [15]. The recombination processes and volt-ampere characteristics have resulted in an increase in the output current, which is good compared to the few voltages used, which give good results for generating light.

In this article, we present a comprehensive study of the photoluminescence properties of CdTe NPLs in terms of their lateral size and thickness. It is shown that the luminescence intensity of NPLs depends on the injection temperature of precursors. We also show that the luminescence spectra shift to the long-wavelength region with an increasing temperature due to an increase in the thickness of the NPL. The dependence of the band gap on the thickness of the NPL is shown. The dependence of the concentration of precursors in the reaction mass and the kinetics of NPL growth are shown. The crystal structure of CdTe NPLs was determined using an electron diffraction (ED) pattern method, revealing their cubic crystal structure. For the prospect of using them as a candidate for low-threshold lasing diodes, the current–voltage characteristic of CdTe NPL was obtained.

2. Materials and Methods

Chemicals. Cadmium acetate dihydrate ($\text{Cd}(\text{OAc})_2 \cdot 2(\text{H}_2\text{O})$), (>98%), 1-octadecene (90% ODE), tellurium powder (98% Te), oleic acid (90% OA), propionic acid (99%), trioctylphosphine (95% TOP), hexane (95%), ethanol (95%), acetone, and liquid azote were used.

All the chemicals used were of the highest purity and were purchased from Sigma-Aldrich Chemie GmbH or Merck. They were used without further purification.

CdTe NPL samples were synthesized using the high-temperature method of pulsed nucleation at 180 °C for 30 min in a high-boiling-temperature solvent according to the modified procedure [4,5,19,23]. Here, Cadmium acetate dihydrate ($\text{Cd}(\text{OAc})_2 \cdot 2(\text{H}_2\text{O})$), was used as the cationic precursor, and tellurium powder dissolved in trioctylphosphine at a concentration of 1M (1M TOP-Te) was used as an anionic precursor. Briefly, a mixture containing 0.5 mmol of cadmium precursor, 0.25 mmol of oleic acid, and 10 mL of octadecene was heated to 180 °C under an argon flow. After that, 100 μL of 1 M solution of tellurium in trioctylphosphine (1M TOP-Te) was injected rapidly, and the growth of the NPLs continued for 30 min. Then, 1 mL of OA was injected, and the flask was cooled down to room temperature. The NPLs were precipitated by the addition of an equal volume of acetone, separated by centrifugation, and dissolved in 2 mL of hexane. After two to three cycles of repeated precipitation and redispersion, the solutions of the CdTe NPLs in hexane with minimum impurity content were obtained.

Material characterization. The UV-Vis absorption, photoluminescence (PL), PL excitation (PLE), and temperature dependence of luminescence were determined using a Jasco V 770 (Tokyo, Japan) spectrophotometer and Solar CM 2203 (Minsk, Belarus) spectrofluorimeter. A UV-Vis spectrophotometer with 1 nm resolution in a quartz cell with 1 cm path length was used. In situ PL was performed using an Ocean Optics QE 65 pro (Duiven, Netherlands) with laser radiation with a wavelength of 400–450 nm. Low-resolution transmission electron microscopy (TEM) images were acquired using a JEM 1400 Plus (Tokyo, Japan) Jeol. High-resolution TEM (HRTEM), high-angle annular dark field-scanning transmission electron microscopy (HAADF-STEM), and STEM-energy dispersive X-ray spectroscopy (STEM-EDX) were performed using an FEI Tenai Osiris transmission electron microscope operating at 200 kV. Ligand exchange was characterized using a Fourier-transform infrared spectrometer (FT-IR Jasco 4700). The current-voltage characteristic using a 10 μm Pedot-TiO₂ electrode was obtained on a PalmSens4 potentiostat.

3. Results and Discussion

The optical properties of the CdTe NPLs were observed from aliquots at 5 min and at 30 min of synthesis. The aliquots were purified with acetone and ethanol in equal proportions, centrifuged at 5000 rpm for 10 min, and redispersed in hexane. The purification procedure was repeated three times. The size-selective precipitation methods did not always succeed in removing the other nanoparticles from the solution, which can be seen in the transmission electron microscopy (TEM) images. Therefore, there is some difference between the absorption, excitation, and PL spectra of the aliquots and purified NPL samples.

Figure 1 shows the absorption and photoluminescence (PL) spectra of the CdTe NPL at room temperature. The absorption spectra reveal two distinct exciton absorption peaks, which can be attributed to the quasi-two-dimensional NPL structure of CdTe. The absorption peaks (black curve) correspond to the electron–light hole transition (384 nm and 445 nm) and the electron–heavy hole transition (426 nm and 494 nm), respectively [23]. The PL spectra show a sharp emission peak and a small Stokes shift (4 meV and 7 meV for each peak group). Because CdTe NPLs are only a few nanometers thick, they are much thinner than their side dimensions, NPLs have a very strong thickness dependent quantum confinement effect. The full width at half maximum of the room temperature (PL) photoluminescence spectra measured for the CdTe nanolayers are much narrower than those for the quantum dots. Based on the emission wavelengths located at 428 nm and 503 nm, the CdTe NPL thickness can be determined as 4 ML and 5 ML, respectively. These data also correlate well with the data of other authors [23]. The full width at half maximum (FWHM) is about 9.6 nm for the other samples of the same order, which implies the good thickness uniformity of the CdTe NPL. For the CdTe NPL, the absorption spectrum is shown, corresponding to the samples taken sequentially during CdTe NPL synthesis (30 min in 180 °C). At the initial stages of synthesis, several NPL populations with a thickness of 4–5 ML coexisted simultaneously (Figure 1). After 30 min of synthesis and beyond, the population of 5 ML NPL became dominant. During the synthesis, NPL populations were replaced by others. Probably, thin NPLs disappeared during the reaction, with the gradual formation of thick NPLs [23]. However, it was not possible to obtain large NPL samples at this temperature, so the synthesis temperature must be increased. The NPL thickness depends on the synthesis temperature and precursor concentration.

The positions of the absorption peaks do not depend on the lateral dimensions of the NPL [24]. The positions of the edges of the conduction bands (CB) and the valence band (VB) NPL can be estimated from the energies of the exciton transitions [2].

Based on the principle that each NPL population corresponds to a certain PL, the appearance and disappearance of emissions will indicate a successive change in the NPL population during synthesis.

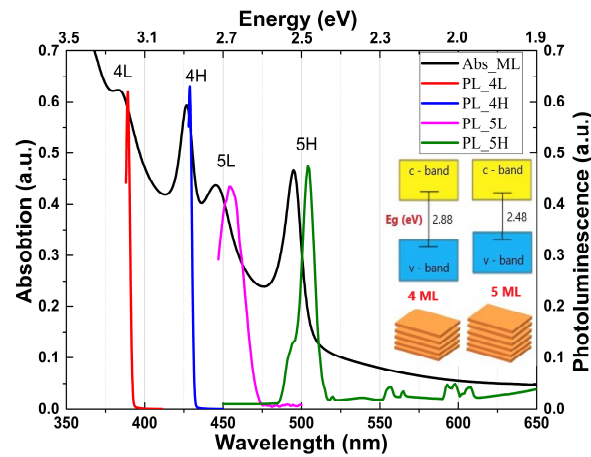


Figure 1. Optical absorption and photoluminescence spectra of CdTe NPL at 180 °C. The 4–5 monolayers; L and H—light and heavy holes, respectively.

As the thickness of the NPL increases, i.e., an increase in the number of mono layers (MLs), the interplane distance between these plates increases. This leads to a shift of the emission and excitation to the long-wavelength region (Figure 1, insert). Accordingly, the band gap width also decreases.

To study the optical properties of CdTe NPL, the temperature dependence of the PL was measured. Figure 2a shows the PL spectra of the aliquots NPL samples at 30 min and 5 min. A Gaussian distribution was observed for the 5 min band (Figure 2a). All the bands belonging to nanoplatelets (2.5 eV) and spherical nanoparticles (2.22 eV) are clearly visible in the figure. Figure 2b shows the PL spectra of in situ synthesis NPL samples. A Gaussian distribution was made for a 30 min band (Figure 2b, insert 1). All bands belonging to the nanoplatelets (2.77 eV), tetrapods (2.39), and spherical nanoparticles (2.04 eV) are clearly visible in Insert 1. The obtained data are consistent with the literature data [1,4,5,25]. The Insert in Figure 2a and Insert 2 in Figure 2b show the PL spectra for the short-wavelength and long-wavelength bands when heated from room temperature and above. It is noted that with an increasing temperature, the intensity of the peak increases, reaching a maximum value at 35–40 °C (Figure 2a) 33 °C, and 45 °C (Figure 2b), and then gradually decreases. For the long-wavelength band, an increase in temperature results in PL quenching. This behavior is typical for all the samples.

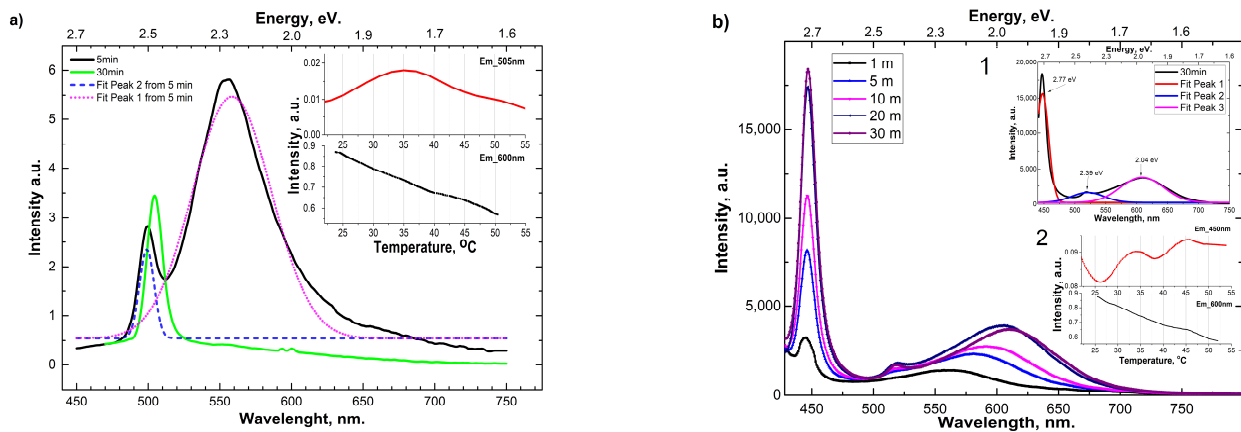


Figure 2. PL spectra of CdTe NPL. (a) Aliquots at 5 (resolved into individual Gaussian components) and 30 min of synthesis at 180 °C. Insert: spectra of temperature dependence of photoluminescence of CdTe NPL samples for the short-wavelength emission band and long-wavelength emission band. (b) In situ synthesis PL spectra of CdTe NPL at 170 °C. Insert (1) sample of 30 min resolved into individual Gaussian components; Insert (2) spectra of temperature dependence of photoluminescence of CdTe NPL samples for the short-wavelength emission band and long-wavelength emission band.

It is known that, for semiconductors, the intensity of photoluminescence will decrease with an increasing temperature due to the thermal release of carriers or thermal activation of nonradiative recombination centers [2]. In Figure 2a,b, for the NPL samples in the temperature range between 35 and 45 °C, there is a slight increase in emissions. According to the authors of [2], this means that more carriers recombine radiatively near the band edge. In the absence of external carriers, this observation can only be attributed to the release of carriers in a localized state (LS) due to the elevated temperature. In addition, the temperature dependence of PL for the long-wavelength band is measured. An increase in temperature from 22 °C to 53 °C leads to emission quenching. This phenomenon can be understood from the proposition that an increase in temperature leads to the disordering of the NPL surface. There is an opinion that the long-wavelength band is related to the features of the NPL surface. The same behavior of the long-wavelength region associated with surface defects and vacancies is characteristic of QDs, for example, CdSe [25].

The homogeneous NPL samples were sensitized. After the injection of precursors, the PL spectra of the aliquots were measured (Figure 3). Analyzing the PL spectra, the dependences of the spectral position of the emission on the number of introduced precursors were plotted.

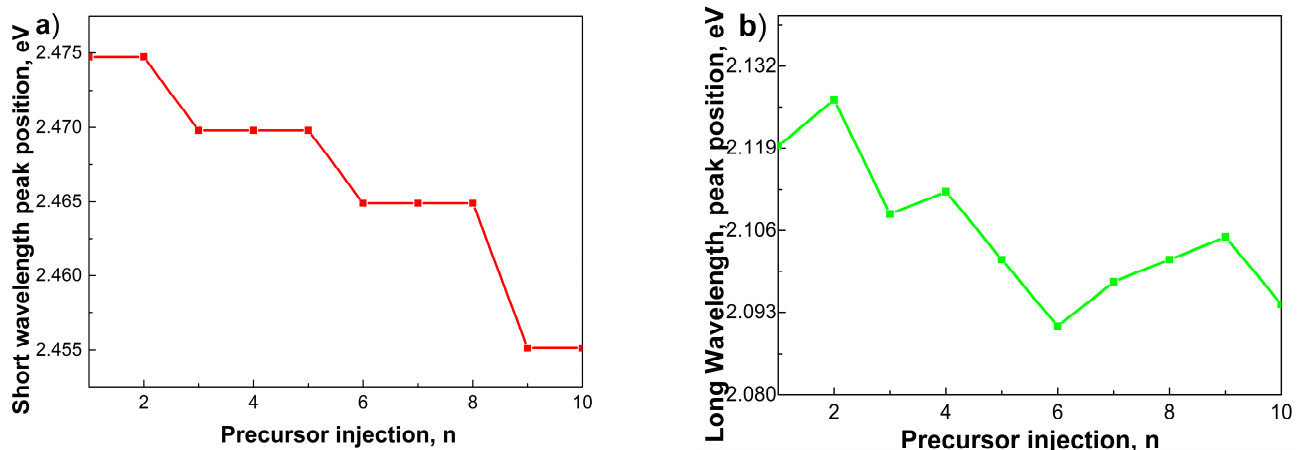


Figure 3. The PL spectra of aliquot in (a) short-wavelength region and (b) long-wavelength region.

For the short-wavelength region, from the general considerations of the formation, maturation, and growth of nanoparticles, considering the literature data [26], we can assume that each injection of precursors caused the further growth of the NPLs. The evidence of such growth is characterized by redshift; hence, there was a decrease in the exciton transition energy.

It is assumed that the shift of the short-wavelength band to the right is associated with an increase in the number of monolayers. As can be seen from Figure 3a, the addition of precursors does not lead to the instantaneous growth of layers; there is a stabilization plateau (steps). The movement of the absorption and emission bands to the right side was synchronous, i.e., accompanied with the preservation of the Stokes shift. At the same time, the long-wavelength band is characterized by a change in position immediately after the injections (Figure 3b). This behavior is characteristic of the growth of CdTe QDs. Usually, QD growth is accompanied by spontaneous growth during precursor injections.

But also, this dependence can be interpreted as the fact that stabilization plateaus (steps) lie within the same structure, and the shift can be due to a small difference in compositions across the layer (from Cd to Te), which is consistent with [26].

It is more difficult to determine the nature of a long-wavelength emission, since its nature can be associated with defects, QD growth, and the lateral growth of nanoplates. These processes can run in parallel and contribute to the emission. This is an interesting area for future research.

Further, it is assumed that with an increase in the synthesis time, the growth step will broaden, i.e., with an increase in the length of the NPL, the step should increase under the condition that the aliquots are taken at equal time intervals. For the best results, in situ synthesis is necessary.

The TEM images in Figure 4 show a square-shaped NPL. The inserts shows the particle size analysis results of the TEM image of the CdTe NPL samples of each of the samples, respectively.

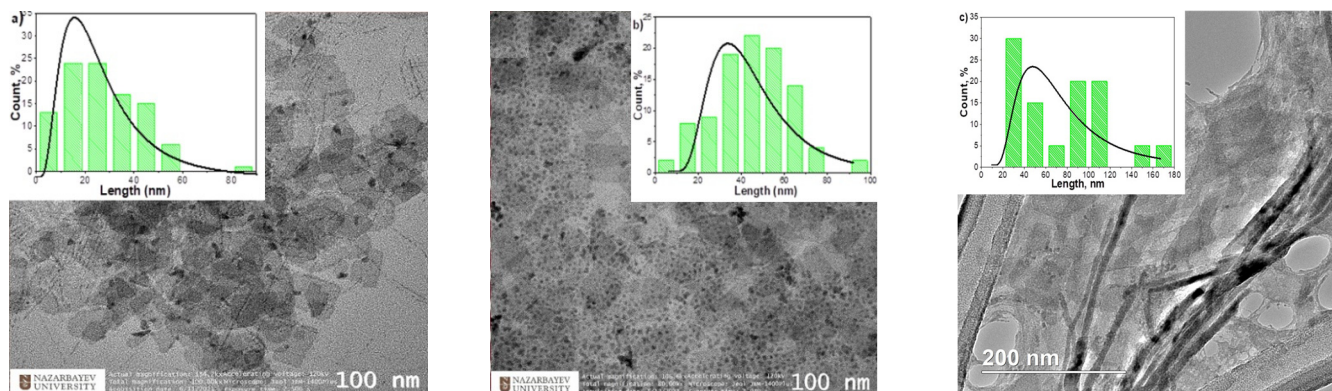


Figure 4. TEM images of CdTe NPL: (a) 5 min aliquots; (b) 30 min aliquots of synthesis; (c) in situ synthesis; inserts: size distribution of the CdTe NPL.

The growth of the NPL is observed on the histograms in the inserts. Sample 1 (5 min aliquot) is dominated by NPLs with a size of 20–30 nm. For sample 2 (30 min aliquot), the lateral growth and, presumably, a slight thickening of the NPL (40–60 nm) upon the addition of precursors, is observed. The NPLs of a small size form large NPLs. Sample 3 (in situ synthesis) is dominated by NPLs with a size of 100–120 nm.

This difference is presumably due to the fact that when taking aliquots, the reaction mass and, accordingly, the growth material decrease.

To further analyze the crystal structure of the as-prepared CdTe NPLs, the selected area electron diffraction (ED) HRTEM pattern of CdTe NPLs shown in Figure 5a was resolved by using the ImageJ tool. Figure 5b shows that the diffraction pattern indicates quasi-single crystalline pattern from the CdTe NPLs. Figure 5c–e presents an HAADF-STEM image and the corresponding STEM-EDX elemental maps of the CdTe NPLs. The element maps show that the obtained NPLs contain both Cd and Te elements, with both elements being evenly distributed throughout the CdTe NPLs. The most pronounced reflections closely match those of cubic CdTe (JCPDS 01-075-2086, Table 1), revealing the zinc blende structure of the NPLs. These results agree with the literature data [5].

Table 1. Lattice spacings of CdTe NPLs fitted by using ImageJ tools.

k (nm^{-1})	Fitted Lattice Spacings d (Å)	Miller Indices (hkl)	Standard Lattice Spacings d (Å) (JCPDS 01-075-2086)	2Theta (Deg)	I (%)
2.54	3.93	(111)	3.70	24.027	0.3
3.06	3.26	(200)	3.20	27.814	100
4.20	2.37	(220)	2.26	39.741	67.7
5.02	1.98	(311)	1.93	46.977	0.1
5.55	1.79	(222)	1.85	49.201	21.8
6.08	1.64	(400)	1.60	57.460	9.3
6.67	1.49	(331)	1.47	63.177	0.1
7.22	1.38	(422)	1.30	72.132	15.5
8.93	1.11	(440)	1.13	85.655	4.1

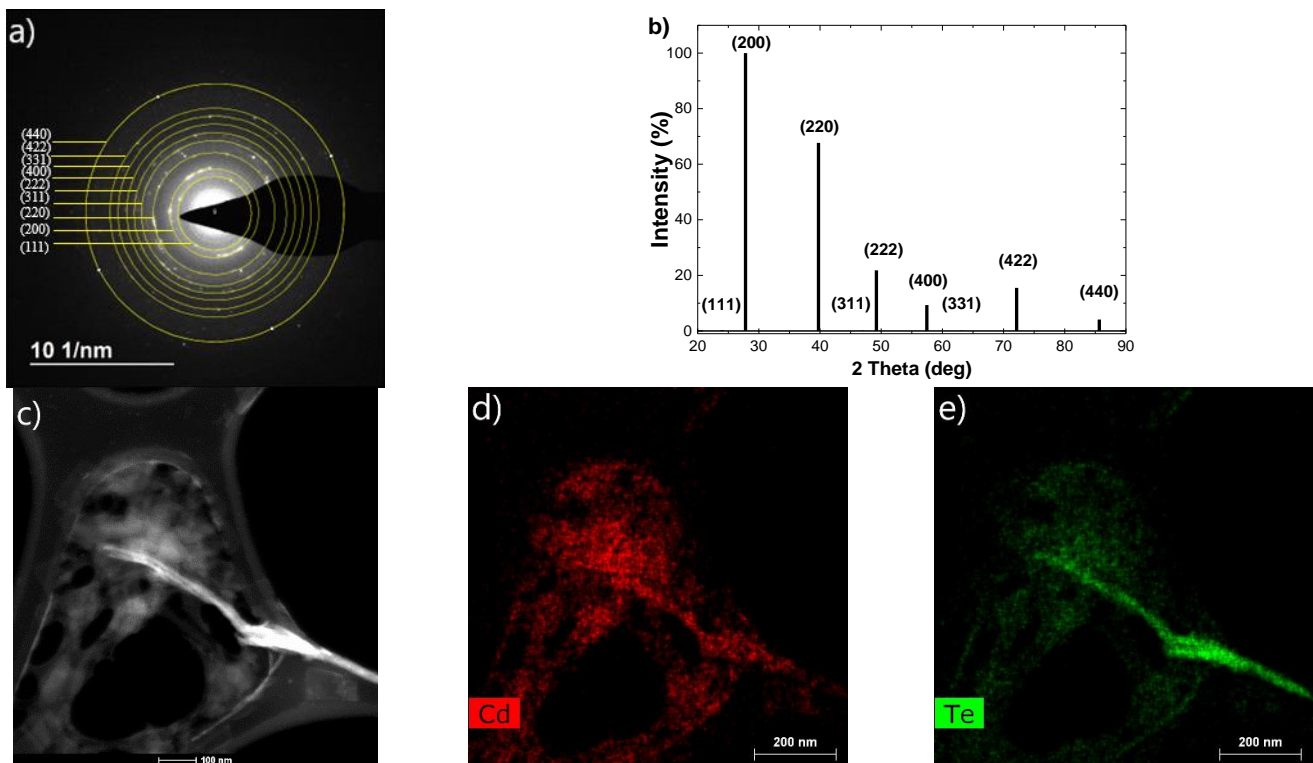


Figure 5. The fitted SAED profile by using ImageJ tools annotated to the original SAED pattern with labeled Miller indices.

Semiconductor NPLs with lateral dimensions are potentially interesting nanoparticles for the construction of devices such as Light-Emitting Diodes, photovoltaic cells, or even photodetectors. This material does not show any measurable conductance as long as the NPLs are capped with an initial oleic acid ligand. On the other hand, after changing the ligand to a shorter TGA ligand, which is also hydrophilic, we can observe a conduction signal. We measured the photoresponse of these CdTe NPL films (Figure 6).

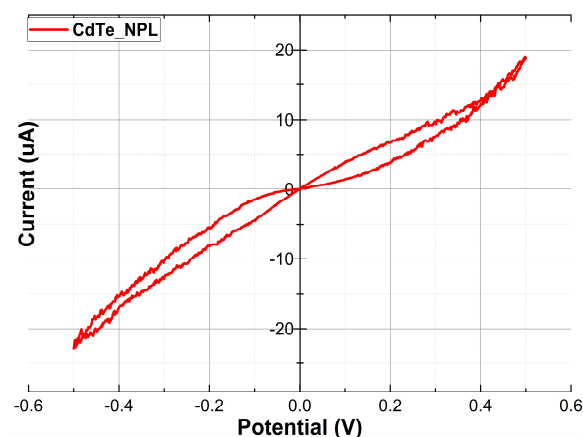


Figure 6. I-V curves under illumination of a film of CdTe NPLs, with an exciton peak at 500 nm.

Figure 6 shows the I-V characteristics of CdTe NPL obtained using the Pedot/TiO₂ electrode. The I-V appearances of the hybrid Pedot/CdTe/TiO₂ device indicate an exponential increase in the current. In a forward bias, the conduction band barrier will shrink due to the exponential distribution of electrons and holes in the conduction and valence bands, and thus, the diffusion current running through the hybrid junction increases exponentially with an increasing forward bias.

4. Conclusions

We have carried out a series of experiments on the synthesis and acquisition of the optical-luminescent characteristics of synthesized CdTe nanoplates at room temperature and under heating.

We assume that the presence of several groups of thicknesses in the absorption spectra indicates that the thickness directly depends on the temperature of the introduction of the precursor anion. The initial temperature was the injection temperature, 160 °C, which was increased to 180 °C for 3–5 min. This is due to four and five monolayer NPLs were formed, respectively.

Our observations of the temperature effect on the NPL dimension showed that the synthesis temperature of 180 °C is insufficient to obtain large NPL samples.

For the first time, the photoluminescence spectrum during the synthesis and growth of NPLs was obtained and studied. The influence of temperature and the concentration of precursors on the thickness of the NPL were assessed.

According to the photoluminescence spectra obtained using two methods, it was found that with the in situ method, NPLs can be obtained in larger sizes, since the reaction mass was taken using the method of selecting aliquots, which reduces the concentration and, accordingly, the size of the NPLs.

We have found that an increase in temperature leads to the disordering of the CdTe NPL surface. According to the PL spectra, the high-energy band should be associated with exciton transitions, while the low-energy band should be assigned to the CdTe NPL surface states, as in semiconductor quantum dots.

The transmission electron microscope (TEM) half-images show various sizes of CdTe NPLs, which supports the theory of the lateral growth of nano wafers. According to the electron diffraction data obtained using a high-resolution transmission electron microscope (HRTEM), the cubic crystal structure of the NPLs was analyzed and revealed.

We have obtained the I-V characteristics of the CdTe NPL, which shows an exponential increase in the current. These results are promising for the future study of NPLs as a candidate for low-threshold-generating diodes.

Comparing the obtained results with the literature data, we can confirm that the thickness depends on the temperature, while the lateral dimensions depend on the concentration and time of synthesis. To obtain large NPLs, it is necessary to increase the temperature and increase the concentration of precursors in the reaction mixture.

Author Contributions: Conceptualization and methodology, A.A., D.D. and A.K.; validation, A.K. and T.N.; investigation, A.A. and B.Y.; data curation, A.K.; writing—original draft preparation, A.A.; writing—review and editing, D.D.; visualization, K.Z.; project administration, A.A. and A.K.; funding acquisition, A.A. and A.K. All authors have read and agreed to the published version of the manuscript.

Funding: This research was funded by the Science Committee of the Ministry of Science and Higher Education of the Republic of Kazakhstan (Grant No AP15473137 and Grant No AP19676416).

Data Availability Statement: The data underlying the results presented in this paper are not publicly available at this time but may be obtained from the authors upon reasonable request.

Acknowledgments: The authors acknowledge M.V. Lomonosov Moscow State University Program of Development for partial support of the instrumental studies. The are also thankful to A.A. Eliseev (Department of Materials Science, M.V. Lomonosov Moscow State University, Moscow, Russian Federation) for the help with I-V characteristics investigation and A.S. Kumskov (Institute of Crystallography, Moscow Russian Federation) for the help with TEM investigations.

Conflicts of Interest: The authors declare no conflict of interest.

References

1. Yu, J.; Chen, R. Optical properties and applications of two-dimensional CdSe nanoplatelets. *InfoMat* **2020**, *2*, 905–927. [[CrossRef](#)]
2. Li, Q.; Lian, T. Area-and thickness-dependent biexciton Auger recombination in colloidal CdSe nanoplatelets: Breaking the “Universal Volume Scaling Law”. *Nano Lett.* **2017**, *17*, 3152–3158. [[CrossRef](#)] [[PubMed](#)]

3. Van Der Bok, J.C.; Dekker, D.M.; Peerlings, M.L.; Salzmann, B.B.; Meijerink, A. Luminescence line broadening of CdSe nanoplatelets and quantum dots for application in w-LEDs. *J. Phys. Chem. C* **2020**, *124*, 12153–12160. [[CrossRef](#)]
4. Pedetti, S.; Nadal, B.; Lhuillier, E.; Mahler, B.; Bouet, C.; Abecassis, B.; Dubertret, B. Optimized synthesis of CdTe nanoplatelets and photoresponse of CdTe nanoplatelets films. *Chem. Mater.* **2013**, *25*, 2455–2462. [[CrossRef](#)]
5. Vasiliev, R.B.; Lazareva, E.P.; Karlova, D.A.; Garshev, A.V.; Yao, Y.; Kuroda, T.; Sakoda, K. Spontaneous folding of CdTe nanosheets induced by ligand exchange. *Chem. Mater.* **2018**, *30*, 1710–1717. [[CrossRef](#)]
6. Noblanc, J.P.; Loudette, J.; Duraffourg, G. Excitonic luminescence of cadmium telluride. *J. Lumin.* **1970**, *1*, 528–541. [[CrossRef](#)]
7. Balakhayeva, R.; Akilbekov, A.; Baimukhanov, Z.; Usseinov, A.; Giniyatova, S.; Zdorovets, M.; Dauletbekova, A. CdTe Nanocrystal Synthesis in SiO₂/Si Ion-Track Template: The Study of Electronic and Structural Properties. *Phys. Status Solidi A* **2021**, *218*, 2000231. [[CrossRef](#)]
8. Akilbekov, A.; Balakhayeva, R.; Zdorovets, M.; Baymukhanov, Z.; Komarov, F.F.; Karim, K.; Dauletbekova, A. Ion track template technology for fabrication of CdTe and CdO nanocrystals. *Nucl. Instrum. Methods Phys. Res. Sect. B Beam Interact. Mater. At.* **2020**, *481*, 30–34. [[CrossRef](#)]
9. Balakhayeva, R.; Akilbekov, A.; Baimukhanov, Z.; Giniyatova, S.; Zdorovets, M.; Gorin, Y.; Dauletbekova, A. Structure properties of CdTe nanocrystals created in SiO₂/Si ion track templates. *Surf. Coat. Technol.* **2020**, *401*, 126269. [[CrossRef](#)]
10. Arivarasan, A.; Bharathi, S.; Essakinaveen, D.; Arunpandiyan, S.; Shanmugapriya, V.; Selvakumar, B.; Jayavel, R. Investigation on the Role of antimony in CdTe QDs sensitized solar cells. *Opt. Mater.* **2022**, *129*, 112551. [[CrossRef](#)]
11. Basak, S.; Das, R. Optical Properties of Synthesized Hexagonal CdTe Nanoparticles Having Hexagonal Phase: Density Functional Theory-Supported Calculation of Bandgap and Density of States. *Phys. Status Solidi B* **2023**, *260*, 2200157. [[CrossRef](#)]
12. Yadav, S.; Malik, P.; Malik, P. CdTe quantum dot-polymer stabilized blue phase liquid crystal nanocomposite with wide blue phase and improved electro-optical responses. *Opt. Mater.* **2023**, *137*, 113608. [[CrossRef](#)]
13. Smirnov, A.M.; Golinskaya, A.D.; Saidzhonov, B.M.; Vasiliev, R.B.; Mantsevich, V.N.; Dneprovskii, V.S. Exciton-exciton interaction and cascade relaxation of excitons in colloidal CdSe nanoplatelets. *J. Lumin.* **2021**, *229*, 117682. [[CrossRef](#)]
14. Deng, D.; Qu, L.; Gu, Y. Controlled transformation of aqueous CdTe quantum dots → Te-rich CdTe nanorods → second CdTe QDs. *RSC Adv.* **2012**, *2*, 11993–11999. [[CrossRef](#)]
15. Kadim, A.M. *Applications of Cadmium Telluride (CdTe) in Nanotechnology. Nanomaterials-Toxicity, Human Health and Environment*; IntechOpen: London, UK, 2019; pp. 1–11. [[CrossRef](#)]
16. Gündoğdu, Y.; Kılıç, H.Ş.; Çadircı, M. Third order nonlinear optical properties of cdte/cdse quasi type-ii colloidal quantum dots. *Opt. Mater.* **2021**, *114*, 110956. [[CrossRef](#)]
17. Wang, F.; Javaid, S.; Chen, W.; Wang, A.; Buntine, M.A.; Jia, G. Synthesis of Atomically Thin CdTe Nanoplatelets by Using Polytelluride Tellurium Precursors. *Aust. J. Chem.* **2020**, *74*, 179–185. [[CrossRef](#)]
18. Anand, A.; Zaffalon, M.L.; Cova, F.; Pinchetti, V.; Khan, A.H.; Carulli, F.; Brovelli, S. Optical and Scintillation Properties of Record-Efficiency CdTe Nanoplatelets toward Radiation Detection Applications. *Nano Lett.* **2022**, *22*, 8900–8907. [[CrossRef](#)]
19. Akhmetova, A.S.; Daurenbekov, D.H.; Kainarbay, A.Z.; Nurakhmetov, T.N.; Eliseev, A.A. Colloidal synthesis of CdTe nanoplatelets using various cadmium precursors. *Opt. Mater.* **2022**, *131*, 112606. [[CrossRef](#)]
20. Yang, F.; Song, P.; Ruan, M.; Xu, W. Recent progress in two-dimensional nanomaterials: Synthesis, engineering, and applications. *FlatChem* **2019**, *18*, 100133. [[CrossRef](#)]
21. Momper, R.; Zhang, H.; Chen, S.; Halim, H.; Johannes, E.; Yordanov, S.; Riedinger, A. Kinetic control over self-assembly of semiconductor nanoplatelets. *Nano Lett.* **2020**, *20*, 4102–4110. [[CrossRef](#)]
22. Meerbach, C.; Wu, C.; Erwin, S.C.; Dang, Z.; Prudnikau, A.; Lesnyak, V. Halide-Assisted Synthesis of Cadmium Chalcogenide Nanoplatelets. *Chem. Mater.* **2019**, *32*, 566–574. [[CrossRef](#)]
23. Ithurria, S.; Tessier, M.D.; Mahler, B.; Lobo, R.P.S.M.; Dubertret, B.; Efros, A.L. Colloidal nanoplatelets with two-dimensional electronic structure. *Nat. Mater.* **2011**, *10*, 936–941. [[CrossRef](#)] [[PubMed](#)]
24. Li, Q.; Lian, T. Exciton spatial coherence and optical gain in colloidal two-dimensional cadmium chalcogenide nanoplatelets. *Acc. Chem. Res.* **2019**, *52*, 2684–2693. [[CrossRef](#)] [[PubMed](#)]
25. Saidzhonov, B.M.; Zaytsev, V.B.; Eliseev, A.A.; Grishko, A.Y.; Vasiliev, R.B. Highly Luminescent Gradient Alloy CdSe_{1-x}S_x Nanoplatelets with Reduced Reabsorption for White-Light Generation. *ACS Photonics* **2020**, *7*, 3188–3198. [[CrossRef](#)]
26. Meulenberg, R.W.; van Buuren, T.; Hanif, K.M.; Willey, T.M.; Strouse, G.F.; Terminello, L.J. Structure and composition of Cu-doped CdSe nanocrystals using soft X-ray absorption spectroscopy. *Nano Lett.* **2004**, *4*, 2277–2285. [[CrossRef](#)]

Disclaimer/Publisher’s Note: The statements, opinions and data contained in all publications are solely those of the individual author(s) and contributor(s) and not of MDPI and/or the editor(s). MDPI and/or the editor(s) disclaim responsibility for any injury to people or property resulting from any ideas, methods, instructions or products referred to in the content.